

Predictive Control Strategies in a Two-Level Voltage Source Inverter

Marco Rivera, José Riveros, Javier Muñoz, Patrick Wheeler

Abstract—In recent years, predictive control has emerged as an alternative for the control of power electronic converters. In this paper, a comparison is presented between the implementation of a predictive current control strategy operating at variable switching frequency and another working at fixed switching frequency. Both strategies use a mathematical model of the converter and load in discrete time in order to predict the behaviour of the load currents and thus choose the switching state that minimizes a given cost function, state which is applied in the next sampling time. The comparison is done based on the percentage of total harmonic distortion (THD) and the error of the output current compared to its reference. The results demonstrate that both techniques work well, but the one operating a fixed switching frequency generates lower ripple and harmonic distortion.

Index Terms—Closed loop systems, DC-AC power converters, Digital control, Predictive control, Prediction methods, Renewable energy sources

I. INTRODUCTION

OVER the past few years, current control in voltage source inverters (VSI) has been an important and researched areas in power electronics. The voltage source inverter is immersed in applications in all types of industries and contexts where this kind of power converter is used [1]. Several methods have been proposed for the control of the VSI, the most common are linear and hysteresis control due to their low implementation complexity [2].

Thanks to new technological advances, the processing speed of microprocessors is improving, allowing the implementation of advanced and more complex control algorithms such as Model Predictive Control (MPC), which has been used in current control for inverters as well as for rectifiers and active filters [3]–[5].

MPC uses a mathematical model of the load and the converter in an intuitive manner to predict the output current and selecting the best state to meet the reference for the following sampling instant. MPC has the advantage and possibility to include nonlinearities in the system and can also be extended to many applications [6], [7].

However, there are some disadvantages associated with the implementation of MPC, such as high computational cost and those related to the finite number of valid switching states. In the absence of a modulator, MPC can produce noise and some oscillations in the voltage and current.

M. Rivera, J. Muñoz. Facultad de Ingeniería, Universidad de Talca, Curicó, Chile (e-mail: marcoriv@utalca.cl, jamunoz@utalca.cl)

J. Riveros. Facultad Politécnica, Universidad Nacional de Asunción, Asunción, Paraguay (e-mail: joservs@gmail.com)

P. Wheeler. Power Electronics, Machines and Control Group, The University of Nottingham, Nottingham, UK (e-mail: Pat.Wheeler@nottingham.ac.uk)

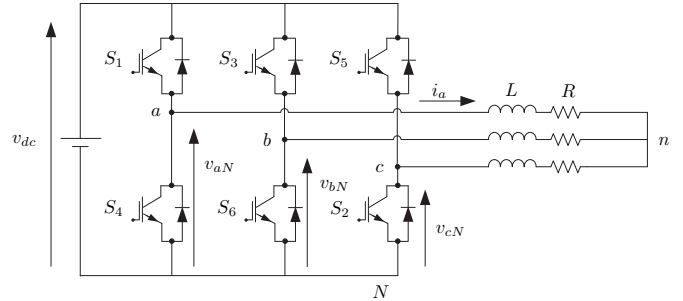


Fig. 1: Topology of the voltage source inverter.

Conventional predictive control techniques generate a spread frequency spectrum, which can decrease the performance of the power converter. Moreover, it requires the use of a filter for a wider frequency range [8], [9]. The literature offers some solutions to the problem of variable frequency in classical predictive control [10], [11]. These include the implementation of a fixed frequency switching strategy, with the modulation of spatial vectors in discrete time within the control algorithm [12] or a conventional modulation within a PI controller [13]. However, these solutions have the problem of complex calculation expressions that are difficult to include into the cost function.

In this paper a predictive control strategy operating at fixed switching frequency which emulates the implementation of space vector modulation (SVM) with a PI linear controller is presented. This technique uses a modulation scheme within the minimization of the cost function which considers a finite number of valid switching states. Working cycles are generated for each vector within a certain sector of the $\alpha - \beta$ plane, which, together with the zero voltage vectors, are applied to the converter using a given pattern sequence. In addition, the conventional predictive current control strategy is presented in order to establish a comparison between both techniques, demonstrating that both strategies allow a good tracking of the load current reference, but the technique operating at fixed switching frequency has a lower ripple and harmonic distortion.

II. TOPOLOGY AND MATHEMATICAL MODEL OF THE VSI

The Voltage Source Inverter (Fig. 1), consists of two fundamental elements, which are the six insulated-gate bipolar transistors (IGBTs) distributed into three legs and a dc-link at the input.

For the current regulation of the load using a model based predictive control (MPC) technique, it is necessary to know the mathematical model that defines the dynamic behavior

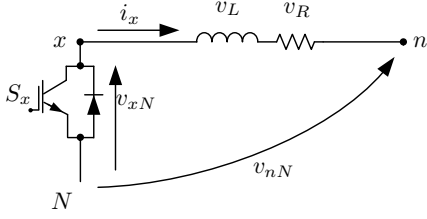


Fig. 2: Simplified VSI mathematical model.

Table I: Available switching states of the VSI.

#	S_1	S_2	S_3	S_4	S_5	S_6	v_{ab}	v_{bc}	v_{ca}	i_{dc}
1	1	1	0	0	0	1	v_{dc}	0	$-v_{dc}$	i_a
2	1	1	1	0	0	0	0	v_{dc}	$-v_{dc}$	$i_a + i_b$
3	0	1	1	1	0	0	$-v_{dc}$	v_{dc}	0	i_b
4	0	0	1	1	1	0	$-v_{dc}$	0	v_{dc}	$i_b + i_c$
5	0	0	0	1	1	1	0	$-v_{dc}$	v_{dc}	i_c
6	1	0	0	0	1	1	v_{dc}	$-v_{dc}$	0	$i_a + i_c$
7	1	0	1	0	1	0	0	0	0	0
8	0	1	0	1	0	1	0	0	0	0

of the system. For this, Kirchhoff's laws is applied to the three-phase load. Fig. 2 shows a simplified model of the system, considering a $R-L$ load and the IGBT switches.

Using Kirchhoff's law, it is possible to obtain the following model of the load:

$$v_{xN} = v_L + v_R + v_{nN} \quad (1)$$

Equation (1) shows a generic model, applicable to the three outputs of the converter. If the following relations for the voltage across the inductance and the resistance are now added,

$$v_L = L \frac{di_x}{dt} \quad (2)$$

$$v_R = Ri_x \quad (3)$$

Equation (1) can now be defined as:

$$v_{xN} = L \frac{di_x}{dt} + Ri_x + v_{nN} \quad (4)$$

Applying equation (4) to the three outputs, an expression for the load voltages can be obtained as:

$$v_{aN} = L \frac{di_a}{dt} + Ri_a + v_{nN} \quad (5)$$

$$v_{bN} = L \frac{di_b}{dt} + Ri_b + v_{nN} \quad (6)$$

$$v_{cN} = L \frac{di_c}{dt} + Ri_c + v_{nN} \quad (7)$$

For the smooth operation of the converter, it is necessary to consider Table I, which contains the eight valid switching states of the VSI. This table also details the line-to-line voltages v_{ab} , v_{bc} y v_{ac} and the dc-link current i_{dc} for each valid switching state.

The eight available switching states are defined based on the operating restrictions of the converter. The dc-link cannot be short circuited and the current in the load cannot be interrupted,

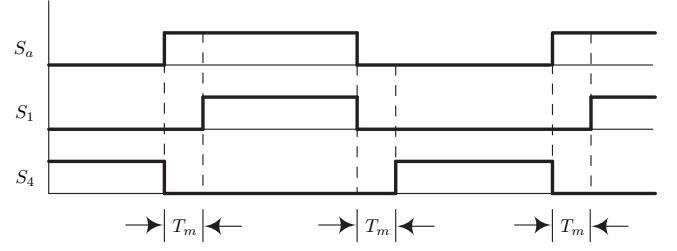


Fig. 3: Dead time applied to the switching of the first leg of the VSI.

thus only one switch per leg must be turned on. This is summarized in:

$$S_a = \begin{cases} 1 & \text{if } S_1 \text{ on and } S_4 \text{ off} \\ 0 & \text{if } S_1 \text{ off and } S_4 \text{ on} \end{cases} \quad (8)$$

$$S_b = \begin{cases} 1 & \text{if } S_3 \text{ on and } S_6 \text{ off} \\ 0 & \text{if } S_3 \text{ off and } S_6 \text{ on} \end{cases} \quad (9)$$

$$S_c = \begin{cases} 1 & \text{if } S_5 \text{ on and } S_2 \text{ off} \\ 0 & \text{if } S_5 \text{ off and } S_2 \text{ on} \end{cases} \quad (10)$$

In order to meet these restrictions and to ensure the safe operation of the converter, a dead time based switching strategy can be implemented. It consists of opening both switches of each leg of the converter at the time of making a change in the value of S_a , S_b or S_c . The opening of the switches is generated for a moment of time " T_m " and is shown in Fig. 3, where the change in S_a occurs.

III. PREDICTIVE CONTROL APPLIED TO THE VSI

Current control in two-level voltage source inverters is an area that is well studied in the field of power electronics. A predictive control strategy applied to the VSI is based on the fact that there is a finite number of possible switching states that can be generated by the power converter. In addition, a system model can be used to predict the behavior of the variables for each switching state. For the choice of the appropriate switching state to be applied at the next sampling time, a cost function g is evaluated, which acts as a state selection criterion. The cost function considers each possible switching state, and then chooses the option that produces the least possible error between the reference and prediction.

A. Predictive current control for the VSI operating at variable switching frequency

The control scheme is shown in Fig. 4. The technique predicts the behavior of the current in the instant of time $k+1$ for each valid switching state, using the dynamic equation that describes the operation of the converter in conjunction with the $R-L$ load. This value is obtained by using the measurements of load currents i_a , i_b , i_c and the dc-link voltage v_{dc} .

Predictive control works with a prediction model implemented in discrete time. Equation (4) defines the system model discretized using the Euler's method, based on a tangential approximation of the derivative:

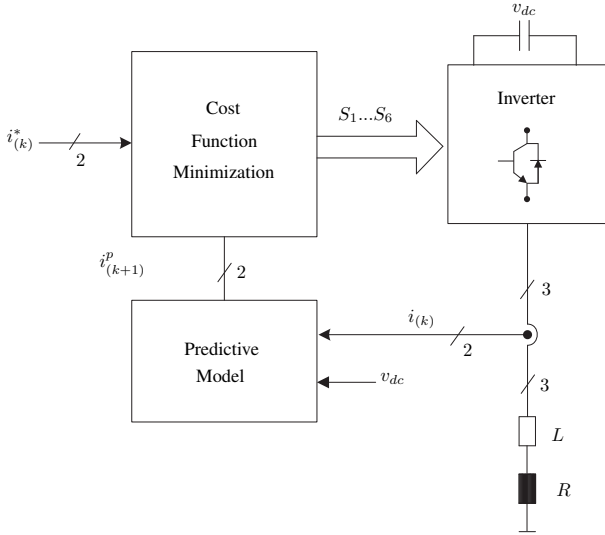


Fig. 4: Block diagram of the control scheme.

$$\frac{di_x}{dt} \approx \frac{i_{k+1} - i_k}{T_s} \quad (11)$$

i_k corresponds to the current value at instant k , i_{k+1} , the predicted current for the next sampling, and T_s is the sampling period. If equation (4) and (11) are combined, the following can be obtained:

$$v_k = L \left[\frac{i_{k+1} - i_k}{T_s} \right] + Ri_k + v_{nN} \quad (12)$$

If the common mode voltage (v_{nN}) is considered as null, a good approximation of the model can be obtained:

$$v_k = L \left[\frac{i_{k+1} - i_k}{T_s} \right] + Ri_k \quad (13)$$

From equation (13) the expression for the load current prediction can be obtained, which is given as a function of the load parameters $R - L$, the measured load current i_k , the prediction of the load voltage (which is given by the dc-link voltage v_{dc}) and the available switching states.

$$i_{k+1} = v_k \left[\frac{T_s}{L} \right] + i_k \left[1 - \frac{T_s R}{L} \right] \quad (14)$$

Knowing the prediction model, the predicted error can be calculated for each valid switching state based on the difference between the reference and the predicted value. This equation is known as the cost function, considering in this case the currents in coordinates $(\alpha - \beta)$ following Clarke's transformation.

The control objective is to select the minimum error between the reference current and the predicted current. When considering the Clarke transform, the currents $(\alpha - \beta)$ are defined according to the output currents i_a, i_b, i_c as follows:

$$i_\alpha = \left[\frac{2i_a - i_b - i_c}{3} \right] \quad (15)$$

$$i_\beta = \left[\frac{i_b - i_c}{\sqrt{3}} \right] \quad (16)$$

The cost function g is as follows:

$$g = [i_\alpha^* - i_\alpha^p]^2 + [i_\beta^* - i_\beta^p]^2 \quad (17)$$

i_α^* and i_β^* are the reference currents in the $\alpha - \beta$ coordinates and i_α^p, i_β^p correspond to the predicted currents of the converter. This function is inserted within a cycle, which evaluates the currents generated by the eight valid switching states and chooses the option that generates the minimum error (minimum value of g).

B. Predictive control of the VSI operating at fixed switching frequency

Classical model predictive control has the particularity of evaluating all the valid switching states of the VSI to predict the current that the converter should have in the following instant to minimize the error and meet the current reference. This process occurs at a variable switching frequency, because the same available switching state could be selected as the optimal during several times. However it is possible also that at every sampling time a different switching state is selected and thus varying the switching frequency, generating ripple and high harmonic distortion in both the load voltage and current. A solution to solve this problem is to use predictive control to emulate the operation of a space vector modulation together with a PI linear controller.

The prediction model used in the classical model predictive control is the same as the one used in the strategy operating at fixed switching frequency. On the other hand, the eight valid switching states of the VSI can be represented in the $\alpha - \beta$ coordinates, considering six available sectors such as shown in Fig. 6.

A model predictive control strategy operating at fixed switching frequency evaluates each sector of the $\alpha - \beta$ plane at every sampling instant, which is composed of two adjacent voltage vectors in addition to a zero vector. The load current predictions are evaluated based on these adjacent vectors, obtaining two cost functions g_1 related to the first vector of

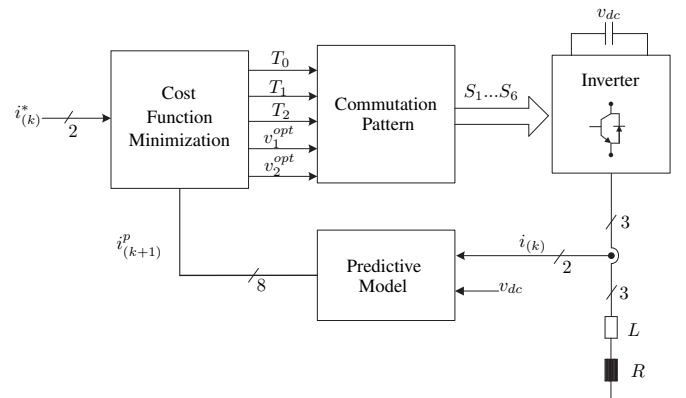


Fig. 5: Block diagram of the predictive current control operating at fixed switching frequency.

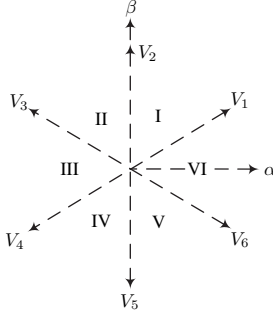


Fig. 6: Vector representation of the available vectors for the VSI.

the sector and g_2 related to the second vector of the sector. This is done at each iteration, evaluating all the sectors in the $\alpha - \beta$ plane, and obtaining different cost functions g_1 and g_2 for each of the six sectors for the VSI. A third cost function g_0 is calculated only once and corresponds to the prediction when switching states producing zero load voltage are applied.

In addition, the different g_1 and g_2 cost functions are used to determine the working cycles that are associated with each vector and can be determined using the following relationships:

$$d_0 = \frac{K}{g_0} \quad (18)$$

$$d_1 = \frac{K}{g_1} \quad (19)$$

$$d_2 = \frac{K}{g_2} \quad (20)$$

$$d_0 + d_1 + d_2 = 1 \quad (21)$$

It is important to highlight that a high value in a cost function, indicates a low duty cycle, which means that the associated vector is applied for less time. By replacing equations (18), (19) and (20) in (21) can be obtained:

$$\frac{K}{g_0} + \frac{K}{g_1} + \frac{K}{g_2} = 1 \quad (22)$$

$$\frac{K g_1 g_2}{g_0 g_1 g_2} + \frac{K g_0 g_2}{g_0 g_1 g_2} + \frac{K g_0 g_1}{g_0 g_1 g_2} = 1 \quad (23)$$

Obtaining the expression for the constant K :

$$K = \frac{g_0 g_1 g_2}{g_1 g_2 + g_0 g_2 + g_0 g_1} \quad (24)$$

and substituting equation (24) into equations (18), (19) and (20):

$$d_0 = \frac{g_1 g_2}{g_1 g_2 + g_0 g_2 + g_0 g_1} \quad (25)$$

$$d_1 = \frac{g_0 g_2}{g_1 g_2 + g_0 g_2 + g_0 g_1} \quad (26)$$

$$d_2 = \frac{g_1 g_0}{g_1 g_2 + g_0 g_2 + g_0 g_1} \quad (27)$$

the new cost function that is optimized (minimized) is determined using the following relationship:

$$g_{(k+1)} = d_1 g_1 + d_2 g_2 \quad (28)$$

The optimal vectors chosen to be applied in the next sampling time to the converter will be those that minimize this new cost function. After the selection of the optimal vectors and, considering the duty cycles, the time T_0 , T_1 and T_2 that each optimal vector is applied can be obtained by:

$$T_0 = T_s d_0 \quad (29)$$

$$T_1 = T_s d_1 \quad (30)$$

$$T_2 = T_s d_2 \quad (31)$$

$$T_s = T_0 + T_1 + T_2 \quad (32)$$

Once the optimal vectors and their times of application have been stated, the switching strategy that will be applied at the next sampling time is established. This commutation strategy can be summarized in seven steps:

- 1) The switching pattern is initiated applying the zero vector, a quarter of its time T_0 ($\frac{T_0}{4}$).
- 2) Then it is applied the first optimal vector v_1^{opt} half of its time T_1 ($\frac{T_1}{2}$).
- 3) Continue applying the second vector v_2^{opt} half of its time T_2 ($\frac{T_2}{2}$).
- 4) Next, the zero vector is applied for a period equivalent to half of its time T_0 ($\frac{T_0}{2}$).
- 5) The second optimal vector v_2^{opt} is applied half of its time T_2 ($\frac{T_2}{2}$).
- 6) The first optimal vector v_1^{opt} is applied half of its half of its time T_1 ($\frac{T_1}{2}$).
- 7) Finally the zero vector is applied, a quarter of its time T_0 ($\frac{T_0}{4}$).

It is important to define which selected vector will be considered as optimum vector one and which one as optimum vector two, in order to ensure that only a change on a single leg of the converter occur. This way the application of the method is optimized and better results are provided. Specifically, for odd sectors (one, three and five) the optimum vector will correspond to the first vector of the sector, considering that the optimal vector will be the one that follows counterclockwise. In the opposite case, for the even sectors (two, four and six), the optimal vector will correspond to the first vector of the sector and the optimal vector will be the one that follows in a clockwise direction. The zero voltage vector can be obtained by two different combinations, the first is when S_1 , S_3 and S_5 are worth zero and the second when S_1 , S_3 and S_5 are worth one. For the correct application of the sequence, the first combination must be applied at the beginning and the end of the sequence, while the application of the zero voltage vector at the middle of the sequence is achieved by applying the second combination. The steps for the implementation of this method are summarized in Fig. 7, where the symmetrical and cyclic performance of the technique can be seen.

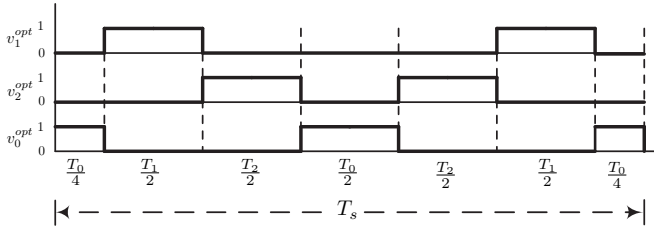


Fig. 7: Switching pattern for the fixed frequency predictive control strategy.

Table II: Simulation parameters of the implementation.

Variables	Description	Value
T_s	Sampling time	100[μ s]
R	Load resistance	10[Ω]
L	Load inductance	10[mH]
v_{dc}	Supply voltage	30[V]
i^*	Reference currents (peak to peak)	0.5[A] y 1[A]
f^*	Frequency of the reference current	25[Hz] y 50[Hz]
	Simulation time	0.1[s]

IV. SIMULATION RESULTS

In order to validate both the predictive current control strategy operating at variable and fixed switching frequency, simulations in Matlab/Simulink have been done using the parameters given in Table II.

Different scenarios have been considering varying the frequency and amplitude of the reference signals. Fig. 8 and Fig. 9 show the results obtained in steady and transient state, respectively. In both figures is observed a good tracking of the load current i_a , i_b to its respective references i_a^* and i_b^* with a fast dynamic response under a step change.

Tables III, IV and V show the comparison of the results obtained in simulation in terms of percentage of harmonic distortion for the voltage v_{an} and for the current i_a , in addition to the steady state error for the current i_a .

In order to obtain a similar response in both predictive techniques, the one operating at variable switching frequency must work at higher sampling frequency than the one operating at fixed switching frequency.

From Table IV, the main differences can be seen when the load current is small with a difference of approximately 10% between both techniques. In terms of steady state error percentage, the predictive technique operating at fixed frequency has better results with lower ripple in the load current. This is because the classical control calculates only an optimal vector during the sampling period at difference of the technique operating at fixed frequency where there are two active vectors and one zero vector applied during the whole sampling period. The predictive control strategy operating at fixed switching frequency generates higher losses, affecting the converter's performance.

V. EXPERIMENTAL RESULTS

In order to validate the results obtained by simulation, a low power prototype has been used. The setup uses the components listed in Table II. The prototype includes a FPGA Bays 2 in

Table III: Percentage of harmonic distortion of the voltage v_{an} in the simulation results.

Frequency	Amplitude	%THD v_{an} Variable Frequency	%THD v_{an} Fixed Frequency
50[Hz]	1[A]	107.15%	108.31%
050[Hz]	0,5[A]	183.79%	192.13%
25[Hz]	1[A]	107.01%	112.16%
25[Hz]	0,5[A]	184.82%	196.77%

Table IV: Percentage of harmonic distortion of the current i_a in the simulation results.

Frequency	Amplitude	%THD i_a Variable Frequency	%THD i_a Fixed Frequency
50[Hz]	1[A]	5.50%	1.26%
50[Hz]	0,5[A]	12.54%	2.61%
25[Hz]	1[A]	5.40%	1.33%
25[Hz]	0,5[A]	11.78%	2.53%

Table V: Percentage of average absolute error of the current i_a in the simulation results.

Frequency	Amplitude	%Error i_a Variable Frequency	%Error i_a Fixed Frequency
50[Hz]	1[A]	4.26%	1.78%
50[Hz]	0,5[A]	4.40%	2.39%
25[Hz]	1[A]	3.29%	1.24%
25[Hz]	0,5[A]	3.54%	1.44%

order to implement the dead time commutation strategy as well as the synchronization with the digital signal processor (DSP). A Delfino F28335 DSP has been used for the implementation of the predictive control techniques.

The experimental results are shown in Fig. 10 and Fig. 11 for steady and transient states, respectively. The experimental results validate the results obtained in the simulations, ensuring sinusoidal load currents with a fast dynamic response. This is also seen in the load voltage v_{an} where is evident that the technique operating at fixed switching frequency has lower harmonic distortion than the load voltage v_{an} obtained with the predictive control technique operating a variable switching frequency.

This result is obtained because the predictive control strategy operating at fixed switching frequency presents an homogeneous commutation sequence, observing load currents with less ripple and a more sinusoidal waveform. In addition, Table VI, VII and VIII detail the comparison of the results obtained experimentally in terms of harmonic distortion percentage for the voltage v_{an} and for the current i_a , in addition to the steady state error for the current i_a .

VI. CONCLUSION

In this paper two predictive control strategies have been implemented in simulation and practically for a two-level voltage source inverter. One predictive control technique operates at variable switching frequency, choosing a single optimal vector at every sampling instant to be applied to the power converter. The second predictive control strategy operates at fixed switching frequency by implementing a commutation sequence with two active vectors and one zero vector. Both techniques work well, obtaining sinusoidal load currents and voltage with fast dynamic response, but the technique operating at fixed switching frequency shows better results with currents and voltage with less ripple and lower harmonic distortion in comparison to the predictive control technique operating at variable switching frequency.

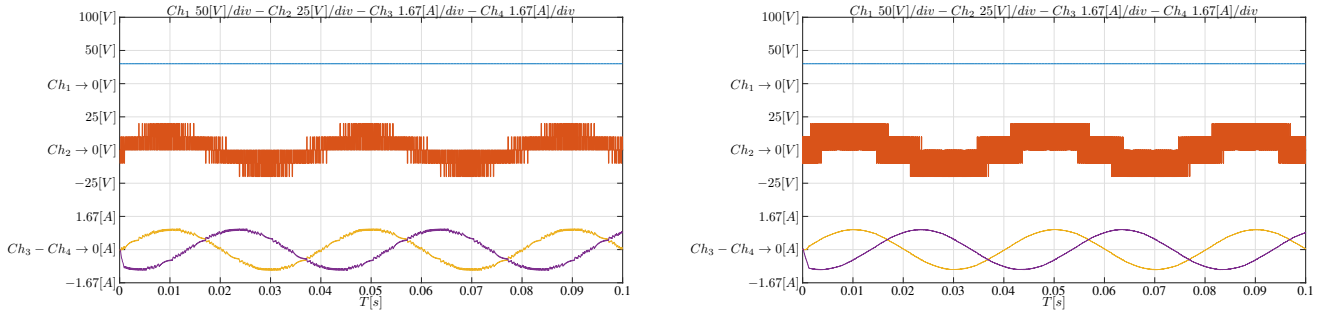


Fig. 8: Simulation results of the predictive control at variable frequency (on the left) and at fixed frequency (on the right) applied to the VSI with a reference of 25[Hz] and 1[A] at steady state. $Ch_1 \rightarrow$ dc voltage (v_{dc}) - $Ch_2 \rightarrow$ phase voltage a (v_{an}) - $Ch_3 \rightarrow$ current in the load (i_a) - $Ch_4 \rightarrow$ current in the load (i_b).

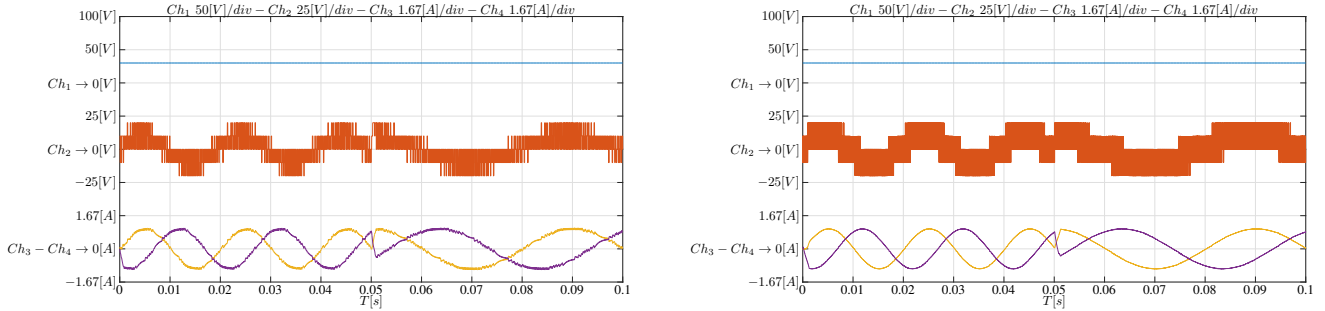


Fig. 9: Simulation results of the predictive control at variable frequency (left) and fixed frequency (right) applied to the VSI with an amplitude of 1[A] and a reference change from 50[Hz] to 25[Hz]. $Ch_1 \rightarrow$ dc voltage (v_{dc}) - $Ch_2 \rightarrow$ phase voltage a (v_{an}) - $Ch_3 \rightarrow$ current in the load (i_a) - $Ch_4 \rightarrow$ current in the load (i_b).

Table VI: Percentage of harmonic distortion of the voltage v_{an} in the experimental results.

Frequency	Amplitude	%THD v_{an} Variable Frequency	%THD v_{an} Fixed Frequency
50[Hz]	1[A]	115.62%	98.40%
50[Hz]	0.5[A]	208.44%	184.99%
25[Hz]	1[A]	121.94%	104.86%
25[Hz]	0.5[A]	210.42%	191.99%

Table VII: Percentage of harmonic distortion of the current i_a in the experimental results.

Frequency	Amplitude	%THD i_a Variable Frequency	%THD i_a Fixed Frequency
50[Hz]	1[A]	10.82%	5.73%
50[Hz]	0.5[A]	22.39%	13.78%
25[Hz]	1[A]	10.46%	6.05%
25[Hz]	0.5[A]	22.80%	18.76%

However, for both cases, there are notable differences between the simulated and experimental results, especially when working with small reference currents. Some of the causes of the differences were the absence of filters at the converter output and mainly the arrangement of the elements within the setup structure. Despite of these differences, has been possible to demonstrate the good performance of the predictive control techniques showing by simulations and experiments that they are a good alternative for the control of power converters.

Table VIII: Percentage of average absolute error of the current i_a in the experimental results.

Frequency	Amplitude	%Error i_a Variable Frequency	%Error i_a Fixed Frequency
50[Hz]	1[A]	6.74%	6.02%
50[Hz]	0.5[A]	8.02%	7.47%
25[Hz]	1[A]	6.85%	5.25%
25[Hz]	0.5[A]	7.62%	7.25%

ACKNOWLEDGMENT

The authors are grateful for the financial support of the FONDECYT Regular Research Project 1191028, Universidad de Talca, The University of Nottingham and FONDAP SERC Chile 15110019.

REFERENCES

- [1] J. Rodriguez and P. Cortes, *Predictive control of power converters and electrical drives*, vol. 40. John Wiley & Sons, 2012.
- [2] H. J., "Pulsewidth modulation for electronic power conversion," *Proc. IEEE*, vol. 82, DOI 10.1109/5.301684, no. 8, pp. 1194–1214, Aug. 1994.
- [3] H. Le-Huy, K. Slimani, and P. Viarouge, "Analysis and implementation of a real-time predictive current controller for permanent-magnet synchronous servo drives," *IEEE Transactions on Industrial Electronics*, vol. 41, no. 1, pp. 110–117, 1994.
- [4] O. Kukrer, "Discrete-time current control of voltage-fed three-phase pwm inverters," *IEEE Transactions on Power Electronics*, vol. 11, no. 2, pp. 260–269, 1996.
- [5] L. Malesani, P. Mattavelli, and S. Buso, "Robust dead-beat current control for pwm rectifiers and active filters," in *Industry Applications Conference, 1998. Thirty-Third IAS Annual Meeting. The 1998 IEEE*, vol. 2, pp. 1377–1384. IEEE, 1998.

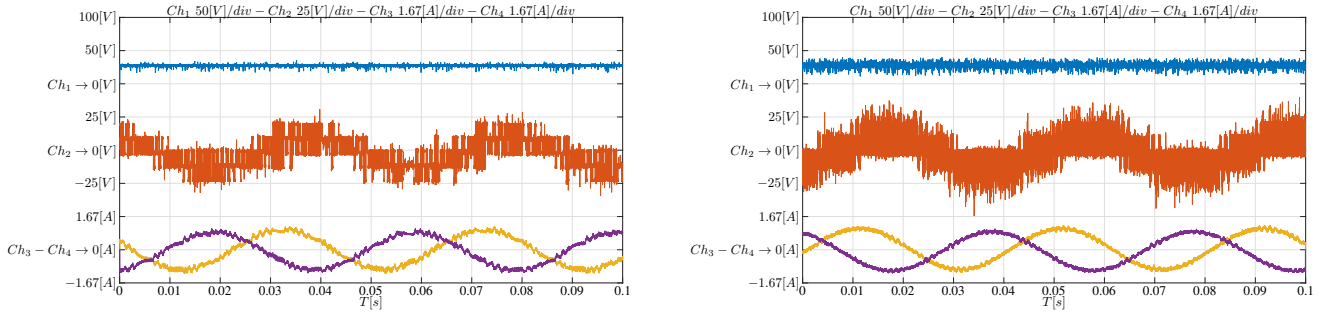


Fig. 10: Experimental results of the predictive control at variable frequency (on the left) and at fixed frequency (on the right) applied to the VSI with a reference of 25[Hz] and 1[A] at steady state. $Ch_1 \rightarrow$ dc voltage (v_{dc}) - $Ch_2 \rightarrow$ phase voltage a (v_{an}) - $Ch_3 \rightarrow$ current in the load (i_a) - $Ch_4 \rightarrow$ current in the load (i_b).

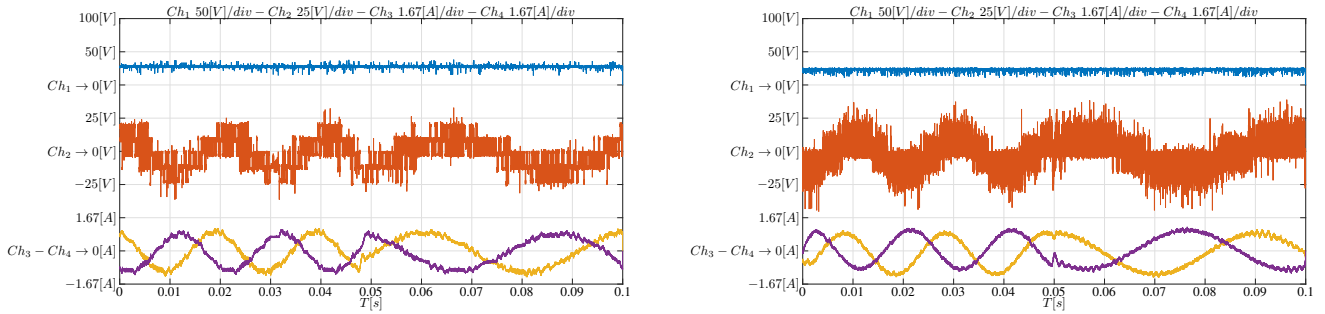


Fig. 11: Experimental results of the predictive control at variable frequency (left) and fixed frequency (right) applied to the VSI with an amplitude of 1[A] and a reference change from 50[Hz] to 25[Hz]. $Ch_1 \rightarrow$ dc voltage (v_{dc}) - $Ch_2 \rightarrow$ phase voltage a (v_{an}) - $Ch_3 \rightarrow$ current in the load (i_a) - $Ch_4 \rightarrow$ current in the load (i_b).

- [6] S. Vazquez, J. I. Leon, L. G. Franquelo, J. Rodriguez, H. A. Young, A. Marquez, and P. Zanchetta, "Model predictive control: A review of its applications in power electronics," *IEEE Industrial Electronics Magazine*, vol. 8, no. 1, pp. 16–31, 2014.
- [7] S. Kouro, P. Cortés, R. Vargas, U. Ammann, and J. Rodríguez, "Model predictive control: A simple and powerful method to control power converters," *IEEE Transactions on industrial electronics*, vol. 56, no. 6, pp. 1826–1838, 2009.
- [8] M. Tomlinson, T. Mouton, R. Kennel, and P. Stolze, "Model predictive control with a fixed switching frequency for an ac-to-ac converter," in *Industrial Technology (ICIT), 2013 IEEE International Conference on*, pp. 570–575. IEEE, 2013.
- [9] R. Mikail, I. Husain, Y. Sozer, M. S. Islam, and T. Sebastian, "A fixed switching frequency predictive current control method for switched reluctance machines," *IEEE Transactions on Industry Applications*, vol. 50, no. 6, pp. 3717–3726, 2014.
- [10] A. Llor, M. Fadel, A. Ziani, M. Rivera, and J. Rodriguez, "Geometrical approach for a predictive current controller applied to a three-phase two-level four-leg inverter," in *IECON 2012-38th Annual Conference on IEEE Industrial Electronics Society*, pp. 5049–5056. IEEE, 2012.
- [11] J. Hu and Z. Zhu, "Improved voltage-vector sequences on dead-beat predictive direct power control of reversible three-phase grid-connected voltage-source converters," *IEEE Transactions on Power Electronics*, vol. 28, no. 1, pp. 254–267, 2013.
- [12] S. Vázquez Pérez, J. I. León Galván, L. García Franquelo, J. M. Carrasco Solís, O. Martínez, J. Rodríguez, P. Cortes, and S. Kouro, "Model predictive control with constant switching frequency using a discrete space vector modulation with virtual state vectors," in *International Conference on Industrial Technology, 1-6. Gippsland, Victoria, Australia: IEEE*, 2009.
- [13] R. Gregor, F. Barrero, S. Toral, M. Duran, M. Arahall, J. Prieto, and J. Mora, "Predictive-space vector pwm current control method for asymmetrical dual three-phase induction motor drives," *IET Electric Power Applications*, vol. 4, no. 1, pp. 26–34, 2010.